A&A 536, A76 (2011)
DOI: 10.1051/0004-6361/201118049
© ESO 2011

Astronomy & Astrophysics

Rotational excitation of 45 levels of ortho/para-H_2O by excited ortho/para-H_2 from 5 K to 1500 K: state-to-state, effective, and thermalized rate coefficients

F. Daniel[1], M.-L. Dubernet[2,3], and A. Grosjean[4]

[1] CAB, INTA-CSIC, Crta, Torrejón km 4, 28850 Torrejn de Ardoz, Madrid, Spain
[2] Observatoire de Paris, LUTH UMR CNRS 8102, 5 Place Janssen, 92195 Meudon, France
e-mail: marie-lise.dubernet@obspm.fr
[3] Université Pierre et Marie Curie, LPMAA UMR CNRS 7092, Case 76, 4 Place Jussieu, 75252 Paris Cedex 05, France
[4] Institut UTINAM, UMR CNRS 6213, 41 bis avenue de l'Observatoire, BP 1615, 25010 Besançon Cedex, France

Received 8 September 2011 / Accepted 10 October 2011

ABSTRACT

Aims. This work deals with the rotational excitation of ortho/para-H_2O with para/ortho-H_2 so that thermalized de-(excitation) rate coefficients up to 1500 K for the first 45th level of ortho/para-H_2O are provided. Results are available in BASECOL with state-to-state rate coefficients, their fitting coefficients, and effective rate coefficients. In addition, we provide a routine that combines all data in order to create thermalized rate coefficients.

Methods. Calculations were performed with the close coupling (CC) method over the whole energy range, using the same 5D potential energy surface (PES) as the one employed in previous papers. The current CC results were compared with thermalized quasi-classical trajectory (QCT) calculations using the same PES and with previous quantum calculations obtained between $T = 20$ K and $T = 140$ K with a different PES. The relative strengths of water excitation rate coefficients when water is excited with ortho-H_2 versus para-H_2 was also analyzed.

Results. For collision with para-H_2, the rotation-rotation process is found to be the dominant process for inelastic transfer for some water transitions, implying that calculations must include the $j_2 = 2$ level. An important result of this paper is that $j_2 = 1$ and $j_2 = 2$ effective rate coefficients are very similar so that either $j_2 = 1$ or $j_2 = 2$ need to be calculated for astrophysical applications. In addition, at high temperature ratios of $j_2 = 2$ (1) over $j_2 = 0$, effective rate coefficients converge towards one to within a few percent. This study confirms that $j_2 = 3$ effective rate coefficients are within 20% to $j_2 = 1$ effective rate coefficients.

Conclusions. For astrophysical applications, these results imply that future collisional excitation of light molecules with H_2 should be carried out with para-H_2, including $j_2 = 2$, so as to obtain correct effective $j_2 = 0$ effective rate coefficients and using the $j_2 = 2$ effective rate coefficients for all excited j_2 effective rate coefficients. In contrast, collisional excitation of heavy molecules with H_2 might be restricted to para-H_2 with $j_2 = 0$ and to ortho-H_2 with $j_2 = 1$, using the $j_2 = 1$ rate coefficients for all excited j_2 effective rate coefficients. These conclusions should simplify the future methodological choice for collisional excitation calculations applied to interstellar/circumstellar media.

Key words. molecular data – molecular processes – ISM: molecules

1. Introduction

This is the fourth (Dubernet et al. 2006b, 2009; Daniel et al. 2010) and last publication from the large-scale effort to obtain the highest possible accuracy for collisional excitation rate coefficients of H_2O with rotationally excited H_2. Those efforts are justified by the importance of water in various astrophysical media. Water is a key molecule for the chemistry and the energy balance of the gas in cold clouds and star-forming regions, thanks to its relatively large abundance and large dipole moment. As the Heterodyne Instrument for the Far-Infrared (HIFI) was launched in May 2009 on board the *Herschel* Space Observatory, publication of the water rate coefficients has become urgent. The instrument has observed the spectra of many molecules with unprecedented sensitivity with an emphasis on water lines in regions such as low- or high-mass star-forming regions, protoplanetary disks, and AGB stars (van Dishoeck et al. 2011; Chavarría et al. 2010; Wyrowski et al. 2010; Bergin et al. 2010; Marseille et al. 2010; Kristensen et al. 2010; Decin et al. 2010). Interpreting these spectra relies upon the accuracy of the available collisional excitation rate coefficients that enter into the population balance of the emitting levels of the molecules. In the temperature range from 5 K to 1500 K, the most abundant collider likely to excite molecules in media with weak UV radiation fields is the hydrogen molecule, followed by the He atom.

The aim of the first paper (Dubernet et al. 2006b) was to study the influence of the new 5D potential energy surface (PES) determined by Faure et al. (2005) and Valiron et al. (2008). This accurate 5D PES, which is suitable for inelastic rotational calculations, was obtained from a 9D PES by averaging over H_2 and H_2O ground vibrational states. As pointed out (Faure et al. 2005; Valiron et al. 2008), this state-averaged PES is actually very close to a rigid-body PES using state-averaged geometries for H_2O and H_2. Dubernet et al. (2006b) showed that this new PES (Faure et al. 2005; Valiron et al. 2008) led to a significant re-evaluation of the rate coefficients for the excitation of H_2O by para-H_2 ($j = 0$) below 20 K and to a weak effect with a maximum change of 40% for collisions with ortho-H_2 ($j = 1$) when their results were compared to the collisional calculations of

Phillips et al. (1996), Dubernet & Grosjean (2002) and Grosjean et al. (2003) obtained with the 5D PES of Phillips et al. (1994). In addition, Dubernet et al. (2006b) provided rate coefficients for de-excitation of the lowest ten rotational levels of o/p-H_2O by collisions with para-H_2 ($j_2 = 0$) and ortho-H_2 ($j_2 = 1$) up to 20 K. This 5D PES has been used for all subsequent (Dubernet et al. 2009; Daniel et al. 2010) calculations, as well as for the present paper.

The second paper (Dubernet et al. 2009) provided state-to-state rate coefficients among the 45 lowest levels of ortho-H_2O with para-H_2 ($j_2 = 0$) and $\Delta j_2 = 0, +2$, as well as with $j_2 = 2$ and $\Delta j_2 = 0, -2$. In addition to and only for the ten lowest energy levels of ortho-H_2O have Dubernet et al. (2009) obtained state-to-state rate coefficients involving $j_2 = 4$ with $\Delta j_2 = 0, -2$ and $j_2 = 2$ with $\Delta j_2 = +2$. The third paper (Daniel et al. 2010) provided state-to-state rate coefficients among the 20 lowest levels of para-H_2O with H_2 ($j_2 = 1$) and $\Delta j_2 = 0, +2$, and among the ten lowest levels of para-H_2O with H_2 ($j_2 = 3$) and $\Delta j_2 = 0, -2$.

In those publications Dubernet et al. (2009), Daniel et al. (2010) carried out comparisons with thermalized QCT calculations of Faure et al. (2007) that shows large factors at intermediate temperatures and factors from 1 to 3 at high temperature for the strongest rate coefficients. We showed also that scaled collisional rate coefficients obtained with He could not be used in place of collisional rate coefficients with para-H_2. The quantum calculations of Dubernet et al. (2009) pointed out the importance of internal energy transfer between excitation of H_2 and de-excitation of ortho-H_2O, which was at the origin of some large differences observed with QCT calculations of Faure et al. (2007) and with scaled collisional rate coefficients obtained with He (Green et al. 1993). We recall that Faure et al. (2007) provides rate coefficients for rotational de-excitation among the lowest 45 rotational levels of o/p-H_2O colliding with thermalized o/p-H_2 in the temperature range of 20 K to 2000 K. This set is a combination of various data: 1) data obtained with quasi classical trajectory (QCT) calculations with the H_2 molecule assumed to be rotationally thermalized at kinetic temperature and calculated between 100 K and 2000 K; 2) the values at 20 K are CC calculations from Dubernet et al. (2006b) for the first five levels and equal to values at 100 K for all other levels; 3) scaled H_2O-He results from Green et al. (1993) for the weakest rate coefficients.

In this paper we provide information on two new systems, i.e. rotational excitation of the 45 lowest levels of ortho-H_2O by ortho-H_2 leading to $j_2 = 1$ effective rate coefficients for the 45 levels and to $j_2 = 3$ effective rate coefficients for the lowest 5 levels. Indeed we provide a limited set of $j_2 = 3$ effective rate coefficients for ortho-H_2O because Daniel et al. (2010) found that ratios of para-H_2O effective rate coefficients $\hat{R}_{j_2=3}/\hat{R}_{j_2=1}$ were generally close to 1 within a maximum variation of 20%. The other new system is para-H_2O-para-H_2 where we provide $j_2 = 0$ and $j_2 = 2$ effective rate coefficients for the 45 and 20 lowest levels respectively. In addition, we complete the (Daniel et al. 2010) calculations providing $j_2 = 1$ effective rate coefficients for rotational de-excitation from the 21rst ($j_\tau = 5_2$) to the 45th ($j_\tau = 7_6$) level of para-H_2O.

2. Methodology

2.1. Collisions with H_2

Our calculations provide state-to-state collisional rate coefficients involving changes in both the target and the perturber rotational levels; i.e. $R(j_1\tau_1 j_2 \rightarrow j'_1\tau'_1 j'_2)(T)$ where $j_1\tau_1$ and $j'_1\tau'_1$ represent the initial and final rotational levels of water, j_2 and j'_2 the initial and final rotational levels of H_2, and T is the kinetic temperature.

The state-to-state collisional rate coefficients are the Boltzmann thermal averages of the state-to-state inelastic cross sections:

$$R(j_1\tau_1 j_2 \rightarrow j'_1\tau'_1 j'_2)(T) = \left(\frac{8}{\pi\mu}\right)^{1/2} \frac{1}{(k_B T)^{3/2}} \int_0^\infty \sigma_{j_1\tau_1 j_2 \rightarrow j'_1\tau'_1 j'_2}(E)\, E\, e^{-E/k_B T}\, dE, \quad (1)$$

where E is the kinetic energy, k_B the Boltzmann constant and μ the reduced mass of the colliding system.

These state-to-state collisional rate coefficients follow the principle of detailed balance, and reverse rate coefficients $R(j'_1\tau'_1 j'_2 \rightarrow j_1\tau_1 j_2)(T)$ can be obtained from forward rate coefficients by the usual formula:

$$g_{j'_1}\, g_{j'_2}\, e^{-\frac{E'_{int}(H_2O)}{k_B T}} e^{-\frac{E'_{int}(H_2)}{k_B T}} R(j'_1\tau'_1 j'_2 \rightarrow j_1\tau_1 j_2) = g_{j_1}\, g_{j_2}\, e^{-\frac{E_{int}(H_2O)}{k_B T}} e^{-\frac{E_{int}(H_2)}{k_B T}} R(j_1\tau_1 j_2 \rightarrow j'_1\tau'_1 j'_2), \quad (2)$$

where g_{j_1} and g_{j_2} are the statistical weights related to rotational levels of H_2O and H_2 respectively, and the different E_{int} are the rotational energies of the species.

Some astrophysical applications might use the so-called effective rate coefficients $\hat{R}_{j_2}(j_1\tau_1 \rightarrow j'_1\tau'_1)$, which are given by the sum of the state-to-state rate coefficients (Eq. (1)) over the final j'_2 states of H_2 for a given initial j_2:

$$\hat{R}_{j_2}(j_1\tau_1 \rightarrow j'_1\tau'_1)(T) = \sum_{j'_2} R(j_1\tau_1 j_2 \rightarrow j'_1\tau'_1 j'_2)(T). \quad (3)$$

These effective rate coefficients do not follow the detailed balance principle, and both excitation and de-excitation should be calculated explicitly.

Finally, averaged de-excitation rate coefficients for ortho/para-H_2O by rotationally thermalized ortho/para-H_2 can be obtained by averaging over the initial rotational levels of ortho/para-H_2:

$$\overline{R}(j_1\tau_1 \rightarrow j'_1\tau'_1) = \sum_{j_2} \rho(j_2)\hat{R}_{j_2}(j_1\tau_1 \rightarrow j'_1\tau'_1)(T) \quad (4)$$

with $\rho(j_2) = g_{j_2} e^{-\frac{E_{int}(H_2)}{k_B T}}/Z$, where Z is the partition function over either ortho/para-H_2 states. These averaged de-excitation rate coefficients are those directly calculated by Faure et al. (2007) with a QCT method.

2.2. Description of the calculations

In the current calculations we used the same expansion of the Faure et al. (2005), Valiron et al. (2008) 5D PES as in Dubernet et al. (2006b), where details can be found. For this PES, inaccuracies in inelastic cross sections might come from different sources: propagation parameters, description of the rotational Hamiltonians of the two molecules, sizes of H_2O and H_2 rotational basis sets, and a level of approximation in quantum calculations where the coupled states (CS) approximation might be used instead of the exact close coupling (CC) method. Additional errors might be introduced in rate coefficients if the kinetic energy grid is not fine enough near thresholds, resulting in poor low-temperature rate coefficients, or not extended to high enough energies, and leading to wrong high-temperature results.

Our quantum calculations were carried out with modified versions of the sequential and parallel versions of the MOLSCAT code (Hutson & Green 1994; McBane 2004). Identical to our previous publications the H_2 energy levels are the experimental energies of Dabrowski (1984), and the H_2O energy levels and eigenfunctions were obtained by diagonalization of the effective Hamiltonian of Kyrö (1981), compatible with the symmetries of the PES. The energy levels of ortho-H_2O and para-H2O can be found in Table 1 of (Dubernet et al. 2009), Table 1 of (Daniel et al. 2010), and in Green et al. (1993). The reduced mass of the system is 1.81277373 a.m.u.

Dubernet et al. (2009), Daniel et al. (2010) should be consulted for choosing an appropriate basis set. In the present calculations the ortho–H2O-ortho-H_2 basis set is chosen to be B(n, 3) for the lowest 20 levels of ortho–H2O in order to be coherent with para-H2O-ortho-H_2 calculations of Daniel et al. (2010). A B(n, 2) basis set is chosen for the para-H2O-para-H_2 calculations for the lowest 45 levels of para-H2O, and n corresponds to the number of water closed channels and is equal to ten. The basis set for para-H_2 is limited to $j_2 = 2$ because the $j_2 = 4$ closed channel has a low overall effect (Dubernet et al. 2009), and because the $j_2 = 4$ effective rate coefficients were very similar to the $j_2 = 2$ effective rate coefficients in previous calculations (Dubernet et al. 2009). For rotational excitation from the 21st level to the 45th levels of either para-H_2O or ortho-H_2O with ortho-H_2 a B(n, 1) basis set is used.

The CC calculations were carried out over essentially the whole energy range spanned by the Boltzmann distributions (Eq. (1)). The highest energy point calculated is at 8000 cm^{-1}, and cross sections are extrapolated at higher energy in order to achieve convergence for de-excitation from the highest water energy levels. These extrapolations do not degrade the accuracy of rate coefficients because the concerned cross sections behave regularly. We carefully spanned the energy range above the inelastic channels and added more points in the presence of resonance structures. The energy steps were fixed to 0.1/0.2/0.5/1 cm^{-1} for kinetic energy below 20/40/60/100 cm^{-1}. Above a kinetic energy of 100 cm^{-1} the steps were progressively increased from 1 cm^{-1} to 500 cm^{-1}. The thresholds' grids were slightly relaxed for calculations above the 30th energy level.

We used the methodology described above to calculate sets of state-to-state rate coefficients (Eq. (1)) described in Tables 1 and 2, in the temperature range from 5 K to 1500 K, for de-excitation among the 45 lowest levels of ortho-H_2O/para-H_2O. From the calculated state-to-state rate coefficients, the effective rate coefficients corresponding to $j_2 = 1, 3$ for ortho-H_2O and to $j_2 = 0, 1, 2$ for para-H_2O can be calculated using Eq. (3). It should be noted that state-to-state and effective rate coefficients are identical for the de-excitation from the 21st to 45th levels ortho-H_2O/para-H_2O by ortho-H_2 because we use a B(n, 1) basis set in these calculations.

The BASECOL database (Dubernet et al. 2006a) provides full tables of the rate coefficient sets mentioned in Tables 1 and 2 i.e. sets (1) to (9). In these tables, the expected accuracy of the sets is given, as a function of the initial level of the de-excitation transition.

2.3. Accuracy of results

Apart from the usual checks of convergence with respect to propagation parameters, basis set, and total angular momentum, the state-to-state rate coefficients have been carefully checked by detailed balance. It should be recalled that the quality of rate coefficients at low temperature is linked to the number of energy points close to the molecular thresholds, and we have an excellent energy grid for both $j_2 = 0, 2$ (20 levels of para-H_2O) and $j_2 = 1$ (20 levels of ortho-H_2O).

The maximum values of the estimated errors are given in Table 1 for transitions starting from different levels of ortho-H_2O and for the various sets of state-to-state rate coefficients (1 to 2). Set (2a) shows very good accuracy for transitions among the first ten levels of ortho-H_2O and for transitions from the 11th–20th levels to the first ten levels of ortho-H_2O. Set (2b) has lower accuracy, but this is not a concern because this set does not contribute significantly to the effective rate coefficients. The accuracy of the effective rate coefficients (ER) $\hat{R}_{j_2=1}$ reflects the accuracies of sets (1) and (2).

The maximum values of the estimated errors are given in Table 2 for transitions starting from different levels of para-H_2O and for the various sets of state-to-state rate coefficients (5 to 9). Again the accuracy of the effective rate coefficients (ER) $\hat{R}_{j_2=0,2}$ reflects the accuracies of sets (5) to (8).

3. Discussion

3.1. Influence of para-H_2 excitation on CC effective rate coefficients

The results obtained for ortho-H_2O (Dubernet et al. 2009) are confirmed in the present calculations. We find that the ratios $\hat{R}_{j_2=2}/\hat{R}_{j_2=0}$ can be very high for para-H_2O transitions for which no internal energy transfer occurs between H_2 and para-H_2O; these high ratios are due to the strong long-range part of the PES for $j_2 = 2$. This is particularly true for the weakest transitions for low-lying energy levels of para-H_2O (top left in Fig. 1) for which we observe ratios up to 80 at $T = 20$ K and commonly around 10 at 100 K. We note that those ratios diminish when the temperature increases. After the 45th transition, the $\hat{R}_{j_2=2}/\hat{R}_{j_2=0}$ ratios have a systematic behavior that is greater than one for de-excitation involving small rotational energy gaps, while smaller than one for the transitions with large energy gaps. This effect, particularly strong for the high rotational levels and for temperature below 400 K, reflects the strong rotation-rotation energy transfer occurring for collisions with para-H_2. Indeed, $\hat{R}_{j_2=0}(\alpha \rightarrow \alpha')$ de-excitation effective rate coefficients are strongly influenced by the corresponding state-to-state rate coefficients $R(j_2 = 0 \rightarrow j_2' = 2; \alpha \rightarrow \alpha')$ for all para-H_2O α levels above the opening of the $j_2 = 2$ level of H_2, while $\hat{R}_{j_2=2}(\alpha \rightarrow \alpha')$ effective rate coefficients are mainly influenced by the $R(j_2 = 2 \rightarrow j_2' = 2; \alpha \rightarrow \alpha')$ state-to-state rate coefficients.

The relative strengths of the different collisional mechanisms: rotation-translation, rotation-rotation are illustrated through the behaviors of the state-to-state cross sections in Fig. 2, for the de-excitation transitions from respectively the 4th, 7th, and 16th levels of para-H_2O. Very striking is the de-excitation from the 16th to the 2nd level (part 3a) where we note the strong contribution of the rotation-rotation mechanism (red curve) over the full range of kinetic energies.

3.2. Analysis of ortho-H_2 to para-H_2 ratios

An analysis can be conducted on the ortho-H_2 to para-H_2 ratios of thermalized rate coefficients within CC calculations. Figure 3 illustrates that the ortho-H_2 to para-H_2 ratios of para-H_2O thermalized CC rate coefficients go to one when the temperature increases for all transitions, implying that at high temperatures it is only necessary to calculate rate coefficients with one of the

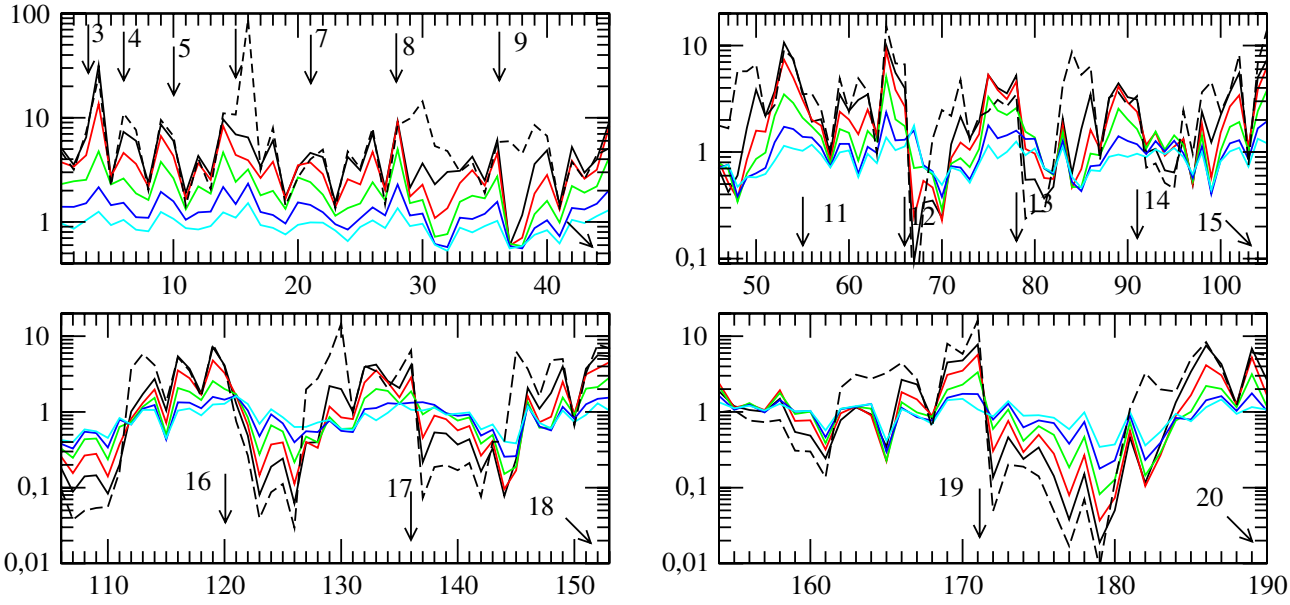

Fig. 1. Ratios of effective de-excitation rate coefficients (Eq. (3)) $\hat{R}_{j_2=2}/\hat{R}_{j_2=0}$ from the 1st to the 190th de-excitation transition and for: T = 20 K (black broken line), T = 100 K (black full line), T = 200 K (red), T = 400 K (green), T = 800 K (blue) and T = 1600 K (cyan). The abscissae indicate the labeling of the de-excitation transitions as indicated in Table 4 of Daniel et al. (2010). The arrows combined with their label "n" indicate the transition $n \rightarrow n-1$.

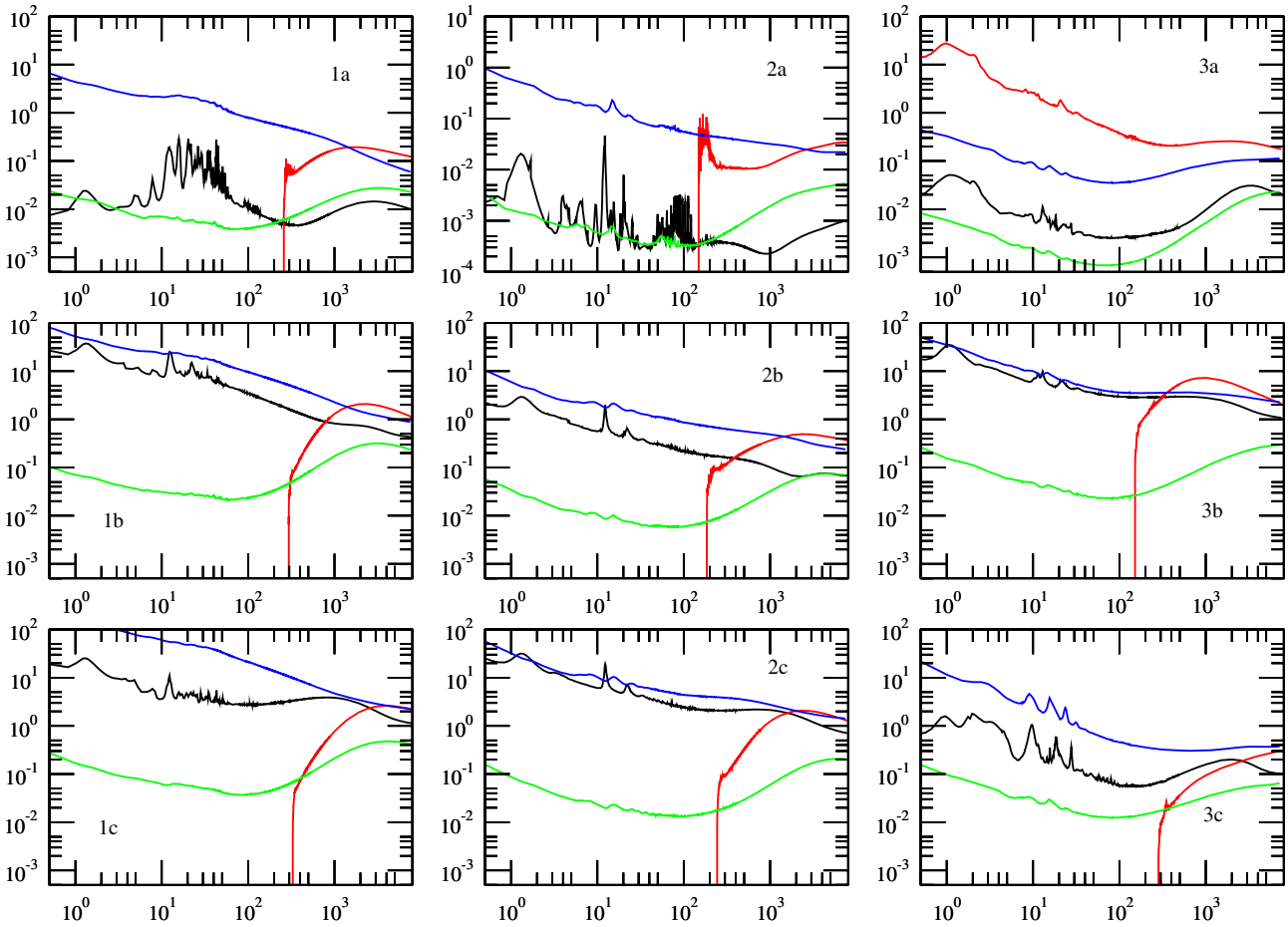

Fig. 2. State-to-state cross-sections in Å^2 as a function of relative kinetic energy (in cm^{-1}) for the para-H_2O transitions: from level $4(2_{11})$ to $1(0_{00})$ **1a)**, to $2(1_{11})$ **1b)**, to $3(2_{02})$ **1c)**; from level $7(3_{22})$ to $1(0_{00})$ **2a)**, to $2(1_{11})$ **2b)**, to $4(2_{11})$; and from level $16(4_{40})$ to $2(1_{11})$ **3a)**, to $10(3_{31})$ **3b)**, to $14(5_{24})$ **3c)**, with the following para-H_2 transitions: $j_2 = 0 \rightarrow j'_2 = 0$ (black), $j_2 = 0 \rightarrow j'_2 = 2$ (red), $j_2 = 2 \rightarrow j'_2 = 0$ (green) and $j_2 = 2 \rightarrow j'_2 = 2$ (blue).

Table 1. Rate coefficients available in BASECOL for ortho-H_2O-ortho-H_2.

Set				T_{min}(K)	T_{max}(K)	Transitions	$T1$	$T2$	$T3$
(1)	$j_2 = 1$	$j'_2 = 1$	STSR	5	1500	45 levels	5%	10%	30%
(2a)		$j'_2 = 3$	STSR	300	1500	20 levels	20%	40%	
(2b)		$j'_2 = 3$	STSR	5	300	20 levels	A2	A2	
		$\sum_{j'2}$	ER	5	1500	45 levels	5%	20%	30%
(3)	$j_2 = 3$	$j'_2 = 3$	STSR	5	1500	5 levels	30 (100) 10		
(4)		$j'_2 = 1$	STSR	5	1500	5 levels	A2		
		$\sum_{j'2}$	ER	5	1500	5 levels	30 (100) 10		

Notes. Summary of the sets of state-to-state rate coefficients (STSR) and effective rate coefficients (ER) available in BASECOL for ortho-H_2O-ortho-H_2, with the temperature range covered (columns T_{min} and T_{max}) and the number of levels among which rate coefficients are provided (column Transitions). The columns $T1$, $T2$, and $T3$ give the expected accuracy for the de-excitation transitions among the 10th, 20th and 45th levels, respectively. For some cases, the accuracy is temperature-dependent and labeled X(Y)Z, which mean X% accuracy below a temperature of $T = Y$ Kelvin and Z% accuracy above $T = Y$ Kelvin. When the accuracy is low but involves negligible rate coefficients we adopt the label A2.

Table 2. Same as Table 1 for the para-H_2O–para-H_2 collisional system.

Set				T_{min}(K)	T_{max}(K)	Transitions	$T1$	$T2$	$T3$
(5)	$j_2 = 0$	$j'_2 = 0$	STSR	5	1500	45 levels	5%	10%	30 (200) 10
(6)		$j'_2 = 2$	STSR	5	1500	45 levels	10%	20%	50 (200) 20
		$\sum_{j'2}$	ER	5	1500	45 levels	10%	50 (200) 20	
(7)	$j_2 = 2$	$j'_2 = 0$	STSR	5	1500	20 levels	10%		
(8)		$j'_2 = 2$	STSR	5	1500	20 levels	10%		
		$\sum_{j'2}$	ER	5	1500	20 levels		30%	30%
(9)	$j_2 = 1$	$j'_2 = 1$	STSR (ER)	5	1500	from 21rst to 45	5%	10%	30 (200) 10

Notes. The columns $T1$, $T2$, and $T3$ give the expected accuracy, for the de-excitation transitions among the 20th, 30th, and 45th levels, respectively. The accuracies written $X(Y)Z$ mean X% accuracy below a temperature of $T = Y$ Kelvin and Z% accuracy above $T = Y$ Kelvin.

H_2 species. This is explained by the ratios of the effective rate coefficients displayed in Figs. 4 to 8. This series of figures show that the ratios of effective rate coefficients $\hat{R}_{j_2=1}/\hat{R}_{j_2=0}$ and $\hat{R}_{j_2=2}/\hat{R}_{j_2=0}$ are similar for all transitions over the whole temperature range with a $\hat{R}_{j_2=2}/\hat{R}_{j_2=1}$ ratio close to one within 35% at 200 K and about 20% at higher temperatures. We observe the same quantitative behaviors of the $\hat{R}_{j_2=2}/\hat{R}_{j_2=1}$ ratios for the de-excitation from the 21st to 45th level of ortho-H_2O.

The other ratios $\hat{R}_{j_2=3}/\hat{R}_{j_2=1}$ and $\hat{R}_{j_2=3}/\hat{R}_{j_2=2}$, are close to one within 30–20%. All these ratios go to one to within a few percent when temperature increases, and this effect corresponds to a low influence by the potential well and by the long-range part of the PES on the dynamics of the collision. For the strongest collisional strengths, the ortho-H_2 to para-H_2 ratios are in general close to one to better than 10% over the whole temperature range.

3.3. Comparison with H_2O + H_2 effective rate coefficients of Phillips et al. (1996)

Comparison with effective rate coefficients of Phillips et al. (1996) can only be performed for the first ten levels of ortho/para-H_2O and for temperatures in the range 20 K to 140 K. It is recalled that between 20 K and 140 K, effective rate coefficients (Eq. (3)) for $j_2 = 1$ are equal to ortho-H_2 thermalized rate coefficients (Eq. (4)) since j_3 is barely populated, whereas thermalized rate coefficients (Eq. (4)) for para-H_2 start to depart from the effective rate coefficients (Eq. (3)) for $j_2 = 0$ around 140 K. The ratios of ortho-H_2O-ortho-H_2 ($j_2 = 1$) effective rate coefficients given in Table 3 do not depend noticeably on temperature (The caption of corresponding table in Daniel et al. (2010) is wrong and should be the same as in Table 3). For the first transition of ortho-H_2O the ratio is very close to one, in a similar way to what was found for the first transition of para-H_2O (Daniel et al. 2010). For the other transitions the new PES of Faure et al. (2005), Valiron et al. (2008) does not induce a significant change in rate coefficients for collision with ortho-H_2.

Table 3. Ratios of our effective o–H_2O/o–H_2 rate coefficients for $j_2 = 1$ over Phillips et al. (1996) rate coefficients.

T (K)	20	40	60	80	100	120	140
Transitions							
2 1	1.08	1.08	1.08	1.08	1.07	1.05	1.03
3 1	1.18	1.15	1.14	1.14	1.14	1.14	1.15
3 2	1.19	1.19	1.19	1.82	1.17	1.15	1.14
4 1	1.41	1.38	1.36	1.34	1.34	1.33	1.33
4 2	1.34	1.31	1.30	1.31	1.34	1.37	1.40
4 3	1.17	1.18	1.18	1.18	1.19	1.20	1.21
5 1	1.29	1.24	1.21	1.22	1.24	1.26	1.29
5 2	1.45	1.44	1.42	1.40	1.39	1.37	1.35
5 3	1.24	1.21	1.21	1.22	1.25	1.28	1.30
5 4	1.25	1.26	1.26	1.26	1.24	1.23	1.21

The ratios of para-H_2O-para-H_2 $j_2 = 0$ effective rate coefficients, given in Table 4, decrease slightly with temperature in a similar way to what was found for the ortho-H_2O–para-H_2 system (Note that the caption of corresponding table in Dubernet et al. 2009 is wrong and should be the same as in Table 4). As already mentioned in Dubernet et al. (2009), this certainly reflects the decreasing influence of the difference between the two different PES (Phillips et al. 1994; Faure et al. 2005) as temperature increases.

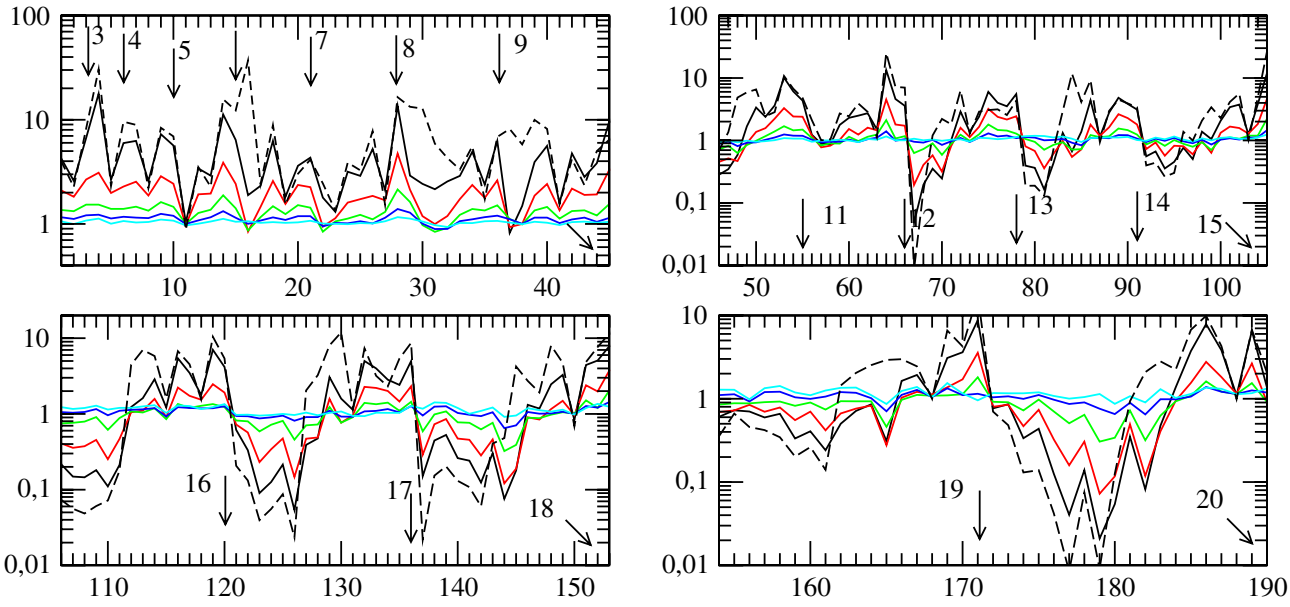

Fig. 3. Ratios of thermalized de-excitation rate coefficients (Eq. (4)) R(ortho-H_2/para-H_2) from the 1st to the 190th de-excitation transition of para-H_2O and for the following temperatures: T = 20 K (back broken line), T = 100 K (black), T = 200 K (red), T = 400 K (green), T = 800 K (blue), and T = 1600 K (cyan). The abscissae indicate the labeling of the de-excitation transitions as given in Table 4 of Daniel et al. (2010). The arrows combined with their label "n" indicate the transition $n \rightarrow n-1$.

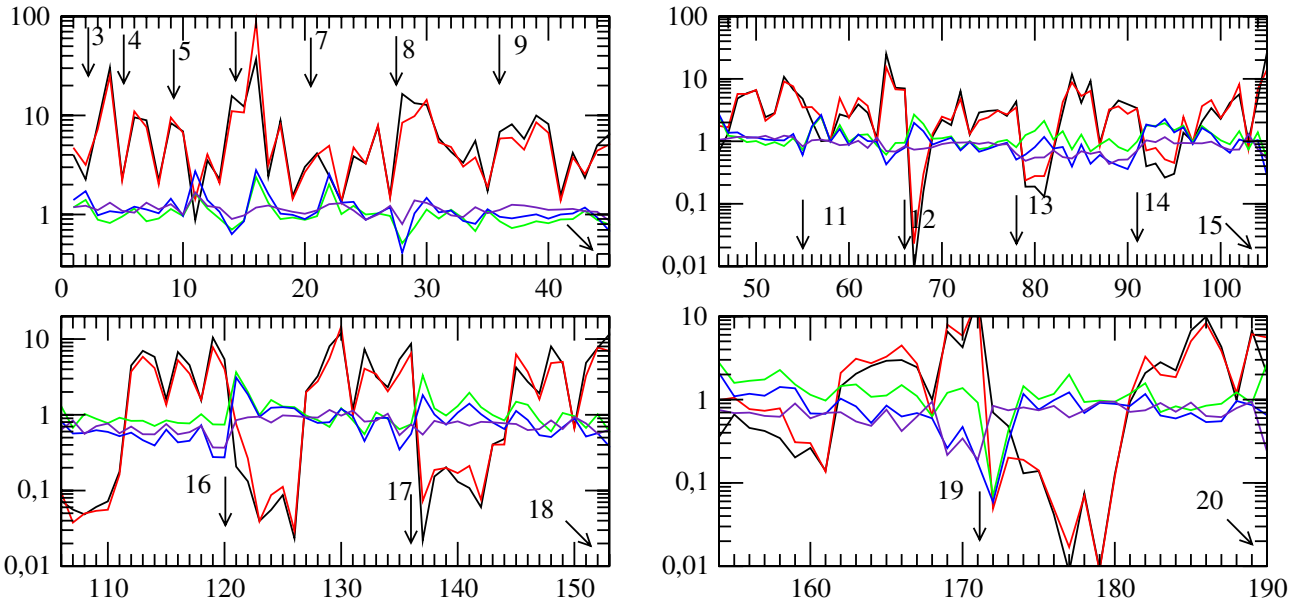

Fig. 4. At T = 20 K, ratios of effective de-excitation rate coefficients (Eq. (3)) from the 1st to the 190th de-excitation transition of para-H_2O: $\hat{R}_{j_2=1}/\hat{R}_{j_2=0}$(black), $\hat{R}_{j_2=2}/\hat{R}_{j_2=0}$ (red), $\hat{R}_{j_2=2}/\hat{R}_{j_2=1}$ (green), $\hat{R}_{j_2=3}/\hat{R}_{j_2=1}$ (blue), and $\hat{R}_{j_2=3}/\hat{R}_{j_2=2}$ (indigo). The abscissae indicate the labeling of the de-excitation transitions as given in Table 4 of Daniel et al. (2010). The arrows combined with their label "n" indicate the transition $n \rightarrow n-1$.

3.4. Fitted rate coefficients

All state-to-state rate coefficients listed in Table 2 and in Table 1 are fitted to an analytical form that is very similar to the one used by Mandy & Martin (1993):

$$\log_{10} R(T) = \sum_{k=1}^{N-1} a_k \left[\log_{10}\frac{T}{\epsilon}\right]^{k-1} + a_N \left(\frac{1}{T/\epsilon+\epsilon} - 1\right), \quad (5)$$

with ϵ and $\{a_k\}_{k\in[1;N]}$ being the fit coefficients. The fits were performed using numerical rate coefficients calculated at ~100 temperatures ranging from $T_{\rm min}$ to $T_{\rm max}$, which are indicated in Tables 1 and 2. The fitted coefficients are such that the maximum error between initial data points and fitted values is minimized. A maximum value of N = 13 is needed for good accuracy over the full range of temperature. The fitted rate coefficients were subsequently compared to numerical rate coefficients calculated with a step of T = 1 K from $T_{\rm min}$ to $T_{\rm max}$, and the maximum error found is less than 0.5%. We emphasize that these fits have no physical meaning, and are only valid in the temperature range of the relevant $T_{\rm min}$, $T_{\rm max}$ and should not be used to perform extrapolations. The complete fitting coefficients (i.e. sets (1) to (4) of Table 1 and (5) to (9) of Table 2) are available in the BASECOL database (Dubernet et al. 2006a). The quality of the fits can be checked online through the graphic interface.

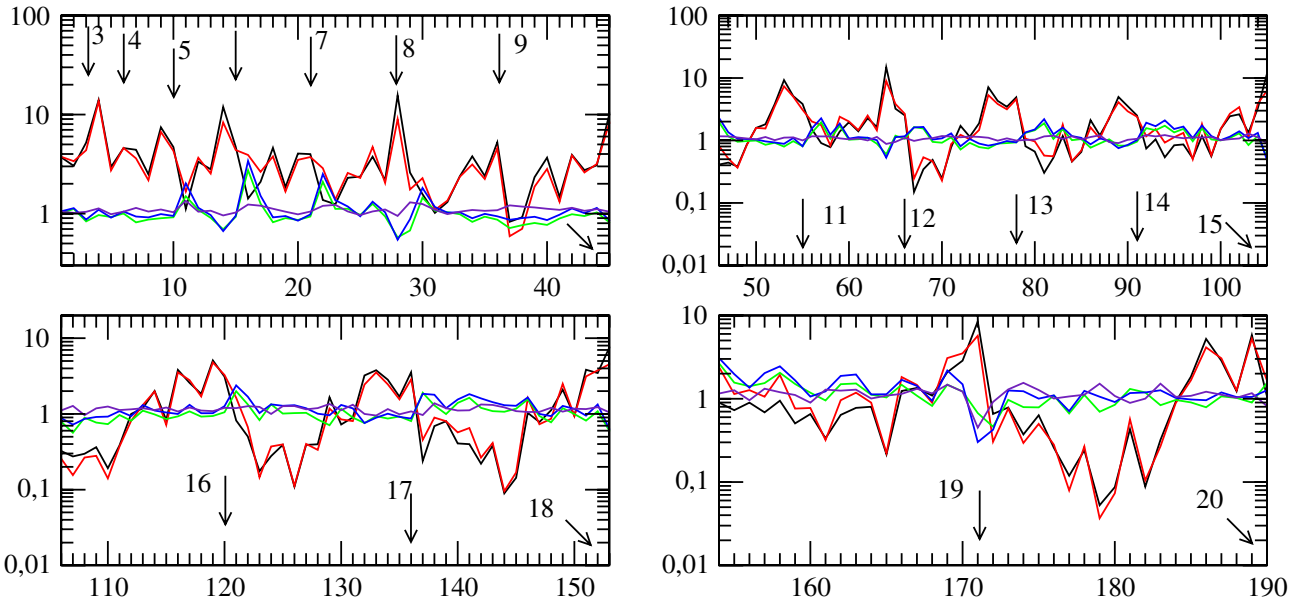

Fig. 5. At $T = 200$ K, ratios of effective de-excitation rate coefficients (Eq. (3)) from the 1st to the 190th de-excitation transition of para-H_2O: $\hat{R}_{j_2=1}/\hat{R}_{j_2=0}$(black), $\hat{R}_{j_2=2}/\hat{R}_{j_2=0}$ (red), $\hat{R}_{j_2=2}/\hat{R}_{j_2=1}$ (green), $\hat{R}_{j_2=3}/\hat{R}_{j_2=1}$ (blue), and $\hat{R}_{j_2=3}/\hat{R}_{j_2=2}$ (indigo). The abscissae indicate the labeling of the de-excitation transitions as given in Table 4 of Daniel et al. (2010). The arrows combined with their label "n" indicate the transition $n \rightarrow n-1$.

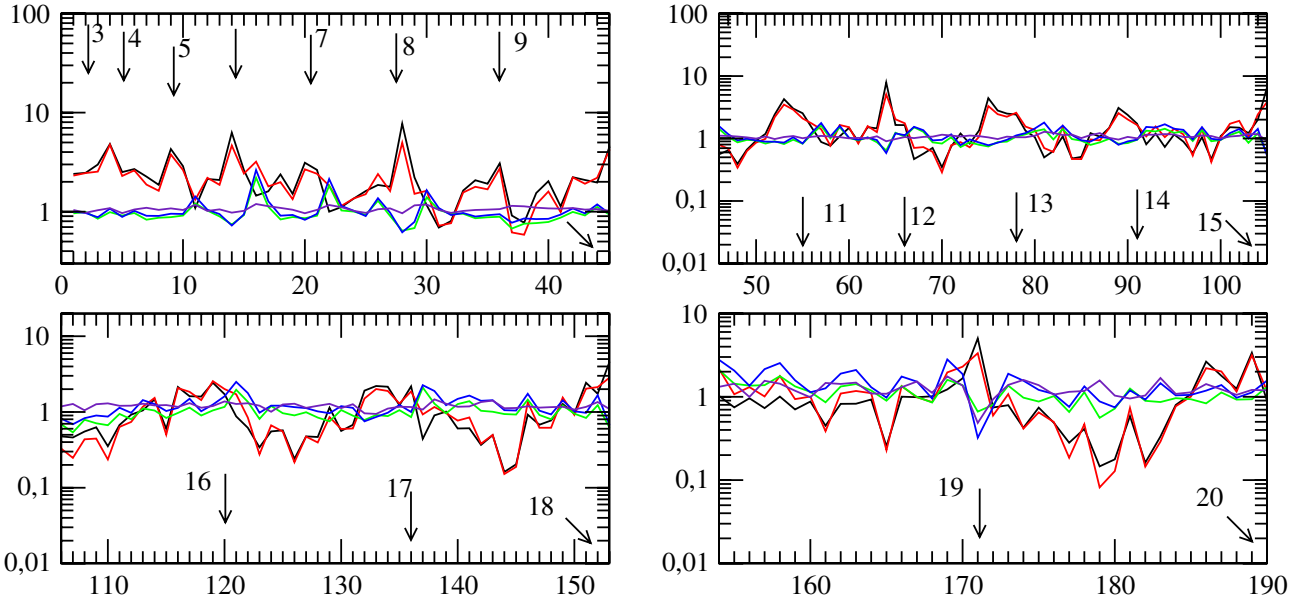

Fig. 6. At $T = 400$ K, ratios of effective de-excitation rate coefficients (Eq. (3)) from the 1st to the 190th de-excitation transition of para-H_2O: $\hat{R}_{j_2=1}/\hat{R}_{j_2=0}$(black), $\hat{R}_{j_2=2}/\hat{R}_{j_2=0}$ (red), $\hat{R}_{j_2=2}/\hat{R}_{j_2=1}$ (green), $\hat{R}_{j_2=3}/\hat{R}_{j_2=1}$ (blue), and $\hat{R}_{j_2=3}/\hat{R}_{j_2=2}$ (indigo). The abscissae indicate the labeling of the de-excitation transitions as given in Table 4 of Daniel et al. (2010). The arrows combined with their label "n" indicate the transition $n \rightarrow n-1$.

3.5. Thermalized rate coefficients and comparison with sets of Faure et al. (2007)

We provide a fortran routine[1] that reads fitting coefficients of all state-to-state rate coefficients calculated in the series of papers Dubernet et al. (2006b, 2009), Daniel et al. (2010), and in the present paper. This routine calculates de-excitation effective rate coefficients for the available possibilities and provides the thermalized de-excitation rate coefficients using both our available effective rate coefficients and guesses based on observations noted in our papers for the non calculated transitions. Table 5 provides an abstract of calculated and estimated effective rate coefficients. The scaling factor M lies between 0.8 and 1.2 for scaling between $\hat{R}(j_2 = 4, 6, 8)$ and $\hat{R}(j_2 = 2)$, between $\hat{R}(j_2 = 3, 5)$ and $\hat{R}(j_2 = 1)$, it should be very close to 1 between $\hat{R}(j_2 = 5)$ and $\hat{R}(j_2 = 3)$ and between $\hat{R}(j_2 = 2)$ and $\hat{R}(j_2 = 1)$. Indeed, we showed in (Daniel et al. 2010) that $j_2 = 3$ significant effective rate coefficients are very close to $j_2 = 1$, therefore we can safely assume all unknown $j_2 = 3, 5, 7$ significant effective rate coefficients to be close to $j_2 = 1$ in calculating the thermalized rate coefficients. We can make the same assumptions concerning all unknown $j_2 = 4, 6, 8$ significant effective rate coefficients with respect to $j_2 = 2$. In addition we showed in the current paper that the $j_2 = 2$ and $j_2 = 1$ effective rate coefficients are very similar. In BASECOL we propose a set of thermalized rate coefficient using $M = 1$.

[1] http://basecol.obspm.fr

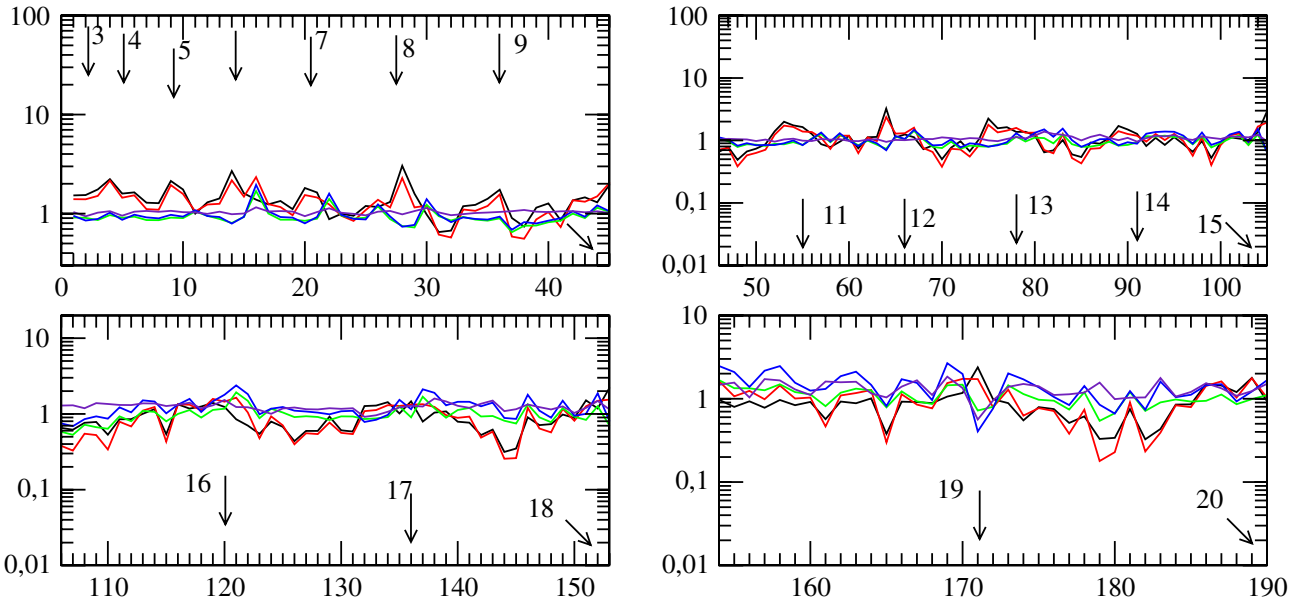

Fig. 7. At $T = 800$ K, ratios of effective de-excitation rate coefficients (Eq. (3)) from the 1st to the 190th de-excitation transition of para-H_2O: $\hat{R}_{j_2=1}/\hat{R}_{j_2=0}$(black), $\hat{R}_{j_2=2}/\hat{R}_{j_2=0}$ (red), $\hat{R}_{j_2=2}/\hat{R}_{j_2=1}$ (green), $\hat{R}_{j_2=3}/\hat{R}_{j_2=1}$ (blue), and $\hat{R}_{j_2=3}/\hat{R}_{j_2=2}$ (indigo). The abscissae indicate the labeling of the de-excitation transitions as given in Table 4 of Daniel et al. (2010). The arrows combined with their label "n" indicate the transition $n \rightarrow n-1$.

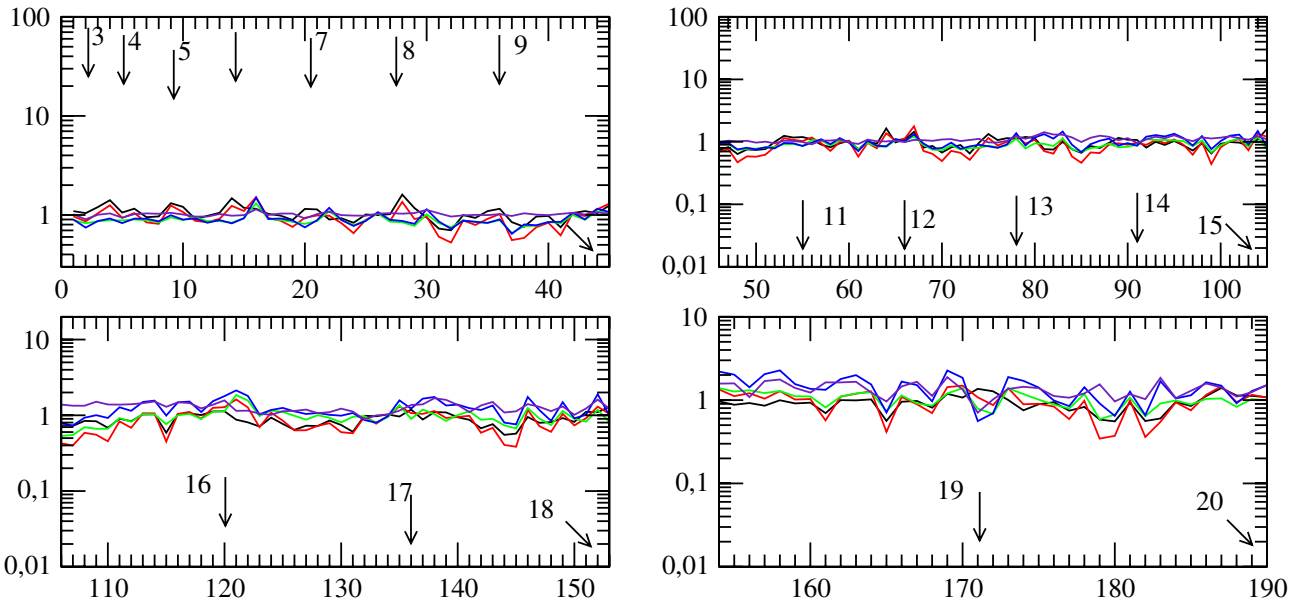

Fig. 8. At $T = 1600$ K, ratios of effective de-excitation rate coefficients (Eq. (3)) from the 1st to the 190th de-excitation transition of para-H_2O: $\hat{R}_{j_2=1}/\hat{R}_{j_2=0}$(black), $\hat{R}_{j_2=2}/\hat{R}_{j_2=0}$ (red), $\hat{R}_{j_2=2}/\hat{R}_{j_2=1}$ (green), $\hat{R}_{j_2=3}/\hat{R}_{j_2=1}$ (blue), and $\hat{R}_{j_2=3}/\hat{R}_{j_2=2}$ (indigo). The abscissae indicate the labeling of the de-excitation transitions as given in Table 4 of Daniel et al. (2010). The arrows combined with their label "n" indicate the transition $n \rightarrow n-1$.

Another possibility for high water levels is to directly use the set of rate coefficients published by Faure et al. (2007), but to be aware of their limitation. Indeed a large fraction of the transitions over a range of temperatures correspond to scaled H_2O-He results of Green et al. (1993) whereas QCT calculations correspond to the most significant rate coefficients (those above 10^{-14}) included in the published sets (Faure et al. 2007). Comparisons between our averaged de-excitation rate coefficients and the QCT results (Faure et al. 2007) have already been performed in previous papers, and the same general conclusions apply to the present calculations. The CC and QCT rate coefficients are within a factor of 3 over the temperature range, whereas scaled He calculations mostly underestimate CC rate coefficients up to several orders of magnitude for the weakest transitions. In addition we note that at low temperatures ortho-H_2 to para-H_2 ratios of thermalized CC rate coefficients behave differently in CC calculations compared to the published set of (Faure et al. 2007). Of course, the scaled-He rate coefficients of Green et al. (1993) included in the published set of Faure et al. (2007) give ratios equal to one. Nonetheless, the ratios involving the QCT rate coefficients differ from the ratios involving CC calculations.

4. Concluding remarks

We have concluded the work on the rotational excitation of ortho/para-H_2O by excited para/ortho-H_2 providing close coupling state-to-state rate coefficients for the lowest 45 levels of ortho/para-H_2O. As indicated in Table 5 some effective rate coefficients need to be guessed for some transitions and range of

Table 4. Ratios of the present para-H_2 rate coefficients with Phillips et al. (1996) $j_2 = 0$ effective rate coefficients.

Transitions/T (K)	20	40	60	80	100	120	140
2 1	1.96	1.81	1.74	1.74	1.84	2.01	2.20
	1.96	1.81	1.73	1.68	1.64	1.60	1.56
3 1	0.86	0.83	0.81	0.81	0.83	0.89	0.98
	0.86	0.83	0.81	0.79	0.77	0.76	0.76
3 2	2.19	1.90	1.77	1.75	1.86	2.07	2.30
	2.19	1.90	1.76	1.67	1.60	1.55	1.51
4 1	2.31	1.90	1.80	2.16	3.34	5.20	7.17
	2.31	1.90	1.74	1.69	1.75	1.87	2.01
4 2	0.86	0.82	0.80	0.79	0.80	0.84	0.89
	0.86	0.82	0.80	0.78	0.77	0.75	0.75
4 3	1.99	1.76	1.68	1.70	1.84	2.07	2.34
	1.99	1.76	1.66	1.60	1.55	1.51	1.49
5 1	1.02	1.03	1.05	1.13	1.32	1.58	1.87
	1.02	1.03	1.04	1.08	1.15	1.22	1.29
5 2	1.44	1.46	1.46	1.47	1.50	1.57	1.65
	1.44	1.46	1.46	1.45	1.44	1.44	1.43
5 3	0.92	0.92	0.94	1.01	1.18	1.46	1.82
	0.92	0.92	0.93	0.94	0.96	0.98	1.01
5 4	1.42	1.46	1.46	1.50	1.64	1.85	2.10
	1.42	1.46	1.45	1.44	1.43	1.42	1.40

Notes. For each transition, the first and second line correspond to ratios involving our thermalized rate coefficients and our $j_2 = 0$ effective rate coefficients (Eq. (3)), respectively.

Table 5. Effective rate coefficients (ER) included in the thermalized rate coefficients.

Transitions/T (K)	CC ER	5 K–140 K	140 K–400 K	400 K–800 K	800 K–1300 K	above
o-H_2O/o-H_2						
up to level 5	$\hat{R}(j_2 = 1, 3)$	OK	OK	OK	OK	$\hat{R}(j_2 = 5) = \hat{R}(j_2 = 3)$
from 6 to 45	$\hat{R}(j_2 = 1)$	OK	OK	$\hat{R}(j_2 = 3) = \hat{R}(j_2 = 1)$	$\hat{R}(j_2 = 3) = \hat{R}(j_2 = 1)$	$\hat{R}(j_2 = 3, 5) = \hat{R}(j_2 = 1)$
o-H_2O/p-H_2						
up to level 10	$\hat{R}(j_2 = 0, 2, 4)$	OK	OK	OK	$\hat{R}(j_2 = 6) = \hat{R}(j_2 = 4)$	$\hat{R}(j_2 = 6, 8) = \hat{R}(j_2 = 4)$
from 11 to 45	$\hat{R}(j_2 = 0,2)$	OK	OK	$\hat{R}(j_2 = 4) = \hat{R}(j_2 = 2)$	$\hat{R}(j_2 = 4, 6) = \hat{R}(j_2 = 2)$	$\hat{R}(j_2 = 4, 6, 8) = \hat{R}(j_2 = 2)$
p-H_2O/o-H_2						
up to level 10	$\hat{R}(j_2 = 1, 3)$	OK	OK	OK	OK	$\hat{R}(j_2 = 5) = \hat{R}(j_2 = 3)$
from 11 to 45	$\hat{R}(j_2 = 1)$	OK	OK	$\hat{R}(j_2 = 3) = \hat{R}(j_2 = 1)$	$\hat{R}(j_2 = 3) = \hat{R}(j_2 = 1)$	$\hat{R}(j_2 = 3,5) = \hat{R}(j_2 = 1)$
p-H_2/p-H_2						
up to level 20	$\hat{R}(j_2 = 0, 2)$	OK	OK	$\hat{R}(j_2 = 4) = \hat{R}(j_2 = 2)$	$\hat{R}(j_2 = 4, 6) = \hat{R}(j_2 = 2)$	$\hat{R}(j_2 = 4, 6, 8) = \hat{R}(j_2 = 2)$
from 21 to 45	$\hat{R}(j_2 = 0)$	OK	$\hat{R}(j_2 = 2) = \hat{R}(j_2 = 1)$	$\hat{R}(j_2 = 2, 4) = \hat{R}(j_2 = 1)$	$\hat{R}(j_2 = 2, 4, 6) = \hat{R}(j_2 = 1)$	$\hat{R}(j_2 = 2, 4, 6, 8) = \hat{R}(j_2 = 1)$

Notes. "OK" indicates that the calculated CC ER are the only significant ER in the corresponding range of temperature. $\hat{R}(j_2 = X) = \hat{R}(j_2 = Y)$ means that $\hat{R}(j_2 = X)$ starts to be significant in the corresponding range of temperature and that it is replaced by the calculated CC ER $\hat{R}(j_2 = Y)$ scaled by a factor M.

temperature. The calculations of these missing effective rate coefficients would have been far too lengthy at the current level of accuracy, thus requiring the use of approximations leading to higher uncertainties in the results. We believe that the uncertainties generated in such approximate calculations would be close to the current guesses, and they are not particularly useful in the context of astrophysical applications. These are educated guesses based on conclusions drawn from comparisons performed between all our calculated sets of CC rate coefficients. Indeed our present results confirm that $j_2 = 3$ calculations are about 20% of $j_2 = 1$, as already been noted by Daniel et al. (2010). Another result of this paper is that $j_2 = 1$ and $j_2 = 2$ effective rate coefficients are very similar so that either $j_2 = 1$ or $j_2 = 2$ need to be calculated for astrophysical applications. Considering that, for some molecule-para-H_2, such as the H_2O systems, rotation-rotation processes are important, it is preferable to carry out scattering calculations with para-H_2 including $j_2 = 0, 2$ in the basis set, so that the $j_2 = 0$ effective rate coefficients are correctly reproduced. The effective $j_2 = 1$ rate coefficients can then be taken as equal to the effective $j_2 = 2$ rate coefficients. On the other hand, for heavy molecules with a high density of rotational states such as CS, SiS, SO_2, and heavier molecules rotation-rotation processes is certainly not efficient with H_2 and calculations might be restricted to para-H_2 with $j_2 = 0$ and to ortho-H_2 with $j_2 = 1$.

In addition at high temperature we find that ratios of $j_2 = 2$ (1) over $j_2 = 0$ effective rate coefficients goes to one to within a few percent, implying that it is enough to calculate the $j_2 = 0$ effective rate coefficients at high temperature. These conclusions should simplify the future methodology choice for the collisional excitation calculations applied to interstellar/circumstellar media.

For citation purposes, the use of each set of state-to-state and related effective rate coefficients data should mention the corresponding collisional paper, the paper of the potential energy surface (Valiron et al. 2008), and the BASECOL database (Dubernet et al. 2006a or a more recent reference) which is the only reference for the numerical values. The use of any thermalized rate coefficients should refer to the potential energy surface (Valiron et al. 2008), and to the complete set of collisional papers (Dubernet et al. 2006b, 2009; Daniel et al. 2010) including the current reference and the BASECOL database (Dubernet et al. (2006a) or a more recent reference).

Table A.1. Example of fit coefficients for the collisional system p-H_2O/p-H_2.

i	i'	j	j'	ϵ	$\{a_k\}_{k\in[1,13]}$						
2	1	1	1	20.	68.3833	0.2532	0.5588	0.4291	0.2774	−0.0287	−0.1900
					−0.0440	0.0544	0.0176	−0.0157	0.0024	82.8438	
2	1	1	2	10.	94.7950	48.4583	−50.1935	41.1937	−23.0060	10.6920	−4.5371
					0.8838	0.2998	−0.1802	0.0247	0.0000	138.8761	
2	1	2	1	11.	53.8859	1.2958	1.0146	0.4899	0.1918	0.0146	0.0985
					−0.6045	0.4228	−0.0823	−0.0086	0.0032	72.8087	
2	1	2	2	6.	−1.1862	0.5561	0.5398	0.1894	−0.6827	0.5465	−0.3331
					0.1244	−0.0018	−0.0165	0.0054	−0.0006	10.1858	
3	1	1	1	7.	−1.6126	0.4469	0.4819	−0.0964	−0.1083	−0.1212	0.1823
					−0.0640	−0.0220	0.0264	−0.0084	0.0009	10.6593	
3	1	1	2	15.	−201.7778	25.5399	−33.1970	23.1147	−13.8836	6.5476	−2.1685
					0.9312	−0.5088	0.1570	−0.0183	0.0000	−190.4983	
3	1	2	1	15.	40.3593	0.6518	0.6724	0.2407	0.1535	0.2679	−0.0749
					−0.2674	−0.0246	0.1950	−0.0907	0.0128	57.0106	
3	1	2	2	13.	−17.4096	0.0402	−0.1020	−0.2382	0.0090	0.1604	−0.0614
					−0.0144	0.0114	−0.0014	−0.0001	0.0000	−7.5226	
3	2	1	1	21.	244.9036	1.1056	1.3441	1.0047	0.4124	−0.0436	0.0323
					−0.3247	−0.1088	0.2866	−0.1186	0.0154	267.7276	
3	2	1	2	14.	−74.0839	32.4889	−38.5675	28.7692	−16.6524	8.1868	−3.0925
					0.7531	−0.0963	0.0042	0.0000	0.0000	−51.6820	

Notes. The label of the initial and final water indexes are i and i' and the H_2 initial and final indexes are j and j', respectively.

Table A.2. Example of fit coefficients for the collisional system o-H_2O/o-H_2.

i	i'	j	j'	ϵ	$\{a_k\}_{k\in[1,13]}$						
2	1	1	1	24.	−17.1866	0.0965	−0.1674	−0.1299	0.1287	0.0235	−0.1328
					0.0702	0.0468	−0.0600	0.0215	−0.0027	−7.9764	
2	1	1	2	13.	−196.4813	60.7381	−74.5234	54.7135	−31.8728	14.8436	−5.4471
					2.4450	−1.3539	0.5042	−0.0964	0.0072	−168.6560	
2	1	2	1	28.	857.9542	2.5996	2.6780	2.2222	1.0094	0.0631	−0.2918
					−0.2372	−0.0122	0.0573	0.0129	−0.0077	902.3999	
2	1	2	2	15.	9.5278	0.2421	0.1273	−0.0607	0.0655	0.2177	−0.1646
					−0.1764	0.2453	−0.1111	0.0226	−0.0017	20.2800	
3	1	1	1	6.	3.6023	0.8263	0.7658	0.2768	−0.4774	−0.0047	−0.0038
					0.0774	−0.0176	−0.0134	0.0063	−0.0008	15.8926	
3	1	1	2	25.	120.2827	30.9700	−34.6723	27.6075	−15.0919	7.3788	−2.9284
					0.6123	−0.1902	0.1908	−0.0796	0.0110	151.8962	
3	1	2	1	40.	413.0149	0.8606	0.8886	1.0111	0.4263	−0.3365	−0.2245
					0.2390	0.0195	−0.0965	0.0284	0.0000	436.9138	
3	1	2	2	10.	−19.4899	0.1639	−0.3835	−0.1337	−0.0778	0.0391	0.4358
					−0.5251	0.2585	−0.0607	0.0057	0.0000	−10.4880	
3	2	1	1	6.	2.3077	0.7565	0.6872	0.1235	−0.1983	−0.5825	0.5876
					−0.1637	−0.0237	0.0240	−0.0053	0.0004	14.3571	
3	2	1	2	14.	−162.7362	55.4103	−66.7295	49.3063	−28.6149	13.4608	−5.0335
					1.7732	−0.5616	0.0816	0.0115	−0.0037	−134.1822	

Notes. The label of the initial and final water indexes are i and i' and the H_2 initial and final indexes are j and j', respectively.

Acknowledgements. Most scattering calculations were performed at the IDRIS-CNRS and CINES under project 2006-07-08-09-10 04 1472. This research was supported by the CNRS national program "Physique et Chimie du Milieu Interstellaire" and by the FP6 Research Training Network "Molecular Universe", contract Number: MRTN-CT-2004-512302. BASECOL is supported by the ASTRONET EU-FP7 Project and by VAMDC funded under the Combination of Collaborative Projects and Coordination and Support Actions Funding Scheme of The Seventh Framework Program. Call topic: INFRA-2008-1.2.2 Scientific Data Infrastructure. Grant Agreement number: 239108. FD thanks Spanish MICINN for support under grant CONSOLIDER ASTROMOL CSD2009-00038 and CSIC for grant JAE-DOC.

Appendix A: Fit coefficients

As said in Sect. 3.4, rate coefficients for the various symmetries of the H_2O/H_2 collisional system are fitted to an analytical form. The fit coefficients are available in the Basecol database Dubernet et al. (2006a) and Tables A.1 and A.2 show a subset of the coefficients, for the actual collisional symmetries. The full tables can be found in the BASECOL database along with a program that enables state-to-state, effective and thermalized rate coefficients to be computed from those coefficients.

References

Bergin, E. A., Hogerheijde, M. R., Brinch, C., et al. 2010, A&A, 521, L33
Chavarría, L., Herpin, F., Jacq, T., et al. 2010, A&A, 521, L37
Dabrowski, I. 1984, Canadian J. Phys., 62, 1639
Daniel, F., Dubernet, M., Pacaud, F., & Grosjean, A. 2010, A&A, 517, A13
Decin, L., Agúndez, M., Barlow, M. J., et al. 2010, Nature, 467, 64
Dubernet, M.-L., & Grosjean, A. 2002, A&A, 390, 793
Dubernet, M., Grosjean, A., Daniel, F., et al. 2006a, in Ro-vibrational Collisional Excitation Database: BASECOL – http://basecol.obspm.fr (Japan: Journal of Plasma and Fusion Research Series, series 7)
Dubernet, M.-L., Daniel, F., Grosjean, A., et al. 2006b, A&A, 460, 323
Dubernet, M.-L., Daniel, F., Grosjean, A., & Lin, C. Y. 2009, A&A, 497, 911
Faure, A., Valiron, P., Wernli, M., et al. 2005, J. Chem. Phys., 122, 221102
Faure, A., Crimier, N., Ceccarelli, C., et al. 2007, A&A, 472, 1029
Green, S., Maluendes, S., & McLean, A. D. 1993, ApJS, 85, 181
Grosjean, A., Dubernet, M.-L., & Ceccarelli, C. 2003, A&A, 408, 1197
Hutson, J. M., & Green, S. 1994, MOLSCAT computer code,version 14 (United Kingdom: Collaborative Computational Project No. 6 of the Science and Engineering Research Council)
Kristensen, L. E., Visser, R., van Dishoeck, E. F., et al. 2010, A&A, 521, L30
Kyrö, E. 1981, J. Mol. Spectrosc., 88, 167
Mandy, M. E., & Martin, P. G. 1993, ApJS, 86, 199
Marseille, M. G., van der Tak, F. F. S., Herpin, F., et al. 2010, A&A, 521, L32
McBane, G. 2004, MOLSCAT computer code, parallel version (USA: G. McBane)
Phillips, T. R., Maluendes, S., McLean, A. D., & Green, S. 1994, J. Chem. Phys., 101, 5824
Phillips, T. R., Maluendes, S., & Green, S. 1996, ApJS, 107, 467
Valiron, P., Wernli, M., Faure, A., et al. 2008, J. Chem. Phys., 129, 134306
van Dishoeck, E. F., Kristensen, L. E., Benz, A. O., et al. 2011, PASP, 123, 138
Wyrowski, F., van der Tak, F., Herpin, F., et al. 2010, A&A, 521, L34